Hierarchical bioinspired architected materials and structures

Ludovico Musenich, Alessandro Stagni, Flavia Libonati*

University of Genoa, Department of Mechanical, Energy, Management and Transportation Engineering, Via all'Opera Pia 15/A, 16145, Genova, Italy

*Corresponding author: flavia.libonati@unige.it

Abstract

Designing new materials that are both lightweight, damage-tolerant, and sustainable is a primary requirement for the advancement of many technological fields. To date, lattice materials appear to be ideal candidates for achieving such multifunctionality at the material scale and leveraging the structural hierarchy can pave the way to amplify their performance. Nature teaches us that, by designing multiscale architectures through a "bottom-up" logic, it is possible to improve and fine-tune the properties of biological building blocks to get robust and multifunctional materials. Yet, we are still far from achieving such a level of perfection that Nature has. In an attempt to narrow this gap and understand the role of hierarchical strategies in lattice structures, we studied, by finite element modeling, 3D hierarchical lattice structures formed by "beam-based" elementary units. Specifically, we selected two types of unit cells with different mechanical behaviors, we combined them into different topological configurations – through hierarchy and engineering approach – and we studied their mechanical behavior under four-point bending loading. The results of this study are twofold: introducing structural heterogeneity by mixing different unit cell types can be beneficial in terms of mechanical properties, while introducing structural hierarchy does not lead to significant improvements in the deformation behavior of the lattice structures analyzed. The latter, however, significantly changes the surface-to-volume ratios of the lattice structures and thus extends their functionality. The evidence found may open new horizons for applications such as heat exchangers, mechanical filters, tissue regeneration scaffolds, energy storage systems, and packaging.

Acronyms

4PB	Four-point bending
FCC	Face centered cubic
FE-	Finite element(s)
H-	Hierarchical
HL	Hierarchical lattice
NH-	Non-hierarchical
NHL	Non-hierarchical lattice
s.r.	Slenderness ratio
s.t.w.	Stiffness-to-weight ratio
SC	Simple cubic
u.c.	Unit cell(s)

Keywords

hierarchy; bio-inspired; lattice; bending-dominated; stretching-dominated; architected materials; structural heterogeneity; multifunctionality; FEM; additive manufacturing

1. Introduction

Synthesizing advanced materials with tailored combinations of physical properties that outperform those of conventional materials is a primary goal of materials science research. Indeed, the design of innovative lightweight, damage tolerant, multifunctional, and sustainable materials is a primary need for the development of many sectors such as aerospace, energy, infrastructure, sports, and biomedicine. Lattice materials, thanks to the development of additive manufacturing techniques and new design software, seem to be ideal candidates to address this challenge [1]–[7]. Unlike other engineering materials, lattice structures are characterized by building blocks formed by spatially repeated elementary units that are interposed between the atomic structure and the "bulk" material. This leads them to behave as structures on the micro-to-meso scale and as homogeneous materials on the macro scale [8]–[10] (see figure 1). By changing the geometrical parameters of the unit cells (u.c.), while keeping the base material unchanged, it is possible to range among a wide gamut of properties such as lightness, stiffness, thermal conductivity, and energy absorption. It is also possible to obtain properties not present in conventional materials, such as negative Poisson ratios and negative thermal expansion coefficients (*i.e.*, meta-properties) [11], [12]. In addition, by introducing heterogeneities in the material that constitutes the u.c., the design degrees of freedom are further expanded [13]–[15]. The versatility and advantages of lattice materials are becoming increasingly evident. Yet, many challenges for their optimal implementation in the functional parts of products remain. One of these is to understand how to exploit structural hierarchy to improve their performances [14], [16]–[18]. Nature, indeed, teaches us that, through bottom-up fabrication of sophisticated multiscale architectures, it is possible to amplify the properties of the building blocks of biological materials and to combine them to achieve robust and multifunctional structures. Bone, wood, nacre, and algae are some remarkable examples of how the physical properties of materials can benefit from hierarchical microstructures [19]–[23]. Over the years, we have been able to effectively apply these concepts to the design of large architectural constructions. The Eiffel Tower is a leading example for all [24]. However, we are still far from achieving such "perfection" at the material level, due to the complexity of the processing-structure-property-performance relationship [25]–[27].

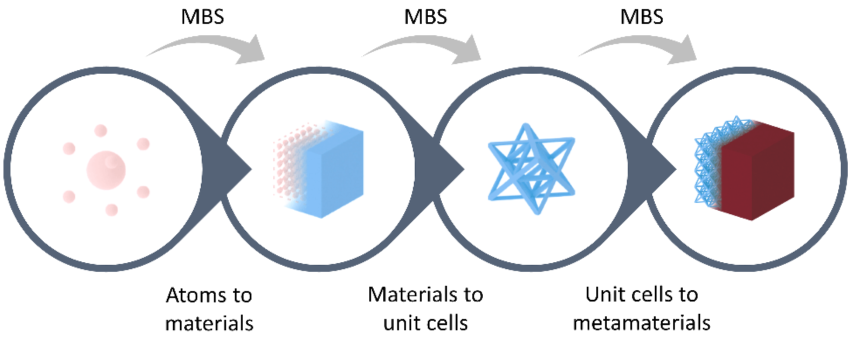

Figure 1 - (a) Material behavior scaling (MBS) scheme for lattice materials. Exploiting a conventional material, by structuring it at the micro/meso scale in the form of a unit cell, allows one to make architected materials that overcome the limitations of conventional materials. Predicting the macroscale performance of lattice materials requires the knowledge of the material properties at each length scale.

In an attempt to reduce this gap and better understand the present relationship between structure and mechanical properties of hierarchical lattice materials, most research has been focused on the analysis of self-similar (or fractal) two-dimensional and three-dimensional strut-based lattice structures [8], [16], [28]–[33]. The apparent mechanical behavior of strut-based lattices can be conventionally described as a function of: i) the properties of the base material, ii) the connectivity of the u.c. (i.e., the number of struts connected at each node), and iii) the relative density (defined as the ratio of the volume of the lattice core to the solid core with identical volume) [9]. Depending on the u.c. connectivity, they have also been classified into two macro-families characterized by distinct mechanical behaviors: *bending-dominated* and *stretching-dominated* structures. The former typically deform through bending of their interconnected members, while the latter deform through compression or uniaxial tension of their members [9], [34]. Their mechanical properties are influenced by their density and by the deformation mode, through the connectivity, and are described by scaling laws. In particular, in terms of elastic modulus, notably, bending-dominated lattices show a quadratic dependence on relative density, while stretching-dominated lattices show a linear one. This means that a bending-dominated lattice material in which the solid parts of the u.c. occupy 10% of the volume is less rigid by a factor of 10 than a stretching-dominated lattice of the same relative density. However, research on the hierarchy effect of the mechanical behavior of such materials has shown that this parameter is not sufficient to fully describe the performance of hierarchical strut-based lattice materials [16], [28]–[34].

To date, we know that by customizing the structural organization of self-similar hierarchical 2D lattice materials, a relatively wide range of elastic properties can be achieved and that some of them can benefit from hierarchical design [28]–[30]. In addition to elastic properties, through multiscale design, crack propagation resistance can also be improved [35]. Similar results have also been found for three-dimensional lattice materials. Specifically, in terms of stiffness, it was observed that bending-dominated lattices benefit from the hierarchy to a greater extent than stretching-dominated ones, while in terms of strength, the presence of more hierarchical levels produces higher stress concentrations that globally reduce the yield strength of the material [31]. Moreover, beyond two levels of hierarchy no appreciable increase in strength or stiffness has been observed, suggesting the idea of an optimal degree for the hierarchy [32]. The mechanical behavior of hierarchical self-similar lattice materials, unlike non-hierarchical ones, was also found to be dependent on the slenderness ratios (*s.r.*) of the struts of the different hierarchical levels and no longer on the relative density [33].

By combining bending-dominated u.c. and stretching-dominated u.c. in hierarchical lattice structures of hybrid type unique properties can also be obtained. In particular, it has been observed that the stiffness and elastic buckling resistance of multiscale bending-bending lattices progressively improve with hierarchy, while for stretching-stretching lattices the increase in buckling resistance is accompanied by a reduction in stiffness. In contrast, bending-stretching lattices showed significant improvement in both stiffness and buckling with hierarchy, while stretching-bending lattices were found to be more flexible but less strong [16]. The behavior of hybrid structures can be further modified by combining together u.c. made of different base materials [32].

In light of previous research results and to extend the current knowledge on the processing-structure-property-performance relationship of multiscale lattice materials, in this work we analyze the specific mechanical performance of 3D hierarchical lattice structures. To evaluate the benefits achievable from exploiting substructures with different behaviors, here we model twelve topologies, by combining two different types of elementary u.c.: bending-dominated and stretching-dominated. Then, through numerical finite element (FE) simulations, we analyze their mechanical behavior as a function of the *s.r.* of the u.c. struts. As a loading scenario we consider the case of a beam subjected to four-point bending (4PB). The bending loading scenario, allows us to work on a simple geometry design space with a gradient stress distribution, guiding the design of lattice structural topologies with the aim of optimal material usage. Furthermore, since in the four-point bending configuration a larger portion of the solid beam is affected by a constant moment, any discontinuities, inherent in lattice structures, are mediated by the larger loaded volume. With our approach we aim to define new mechanical design guidelines for hierarchical lattice structures.

2. Materials and Methods

2.1 Topological design

We consider a 3D 4PB beam as a case study. The design space has a square cross section (H=48 mm) and a length L=192 mm. The pin distances were set to 144 mm and 48 mm for the supports and for the pushing pins, respectively. The design space is voxelized into cubes having 12 mm edge length (figure 2b) that are subsequently populated with different combinations of lattice u.c.: a bending-dominated, the simple cubic (SC), and a stretching-dominated one, the face-centered cubic (FCC). These u.c. are chosen for both their different mechanical behaviors and the excellent geometric compatibility in order to reach a structural heterogeneity in the design space (figure 2a). Starting with the bulk beam, specifically, we model up to three different levels of hierarchy:

i) Level 0, the solid beam (B-beam);
ii) Level 1, the non-hierarchical lattice structure (NHL-structure);
iii) Level 2, the hierarchical lattice structure (HL-structure).

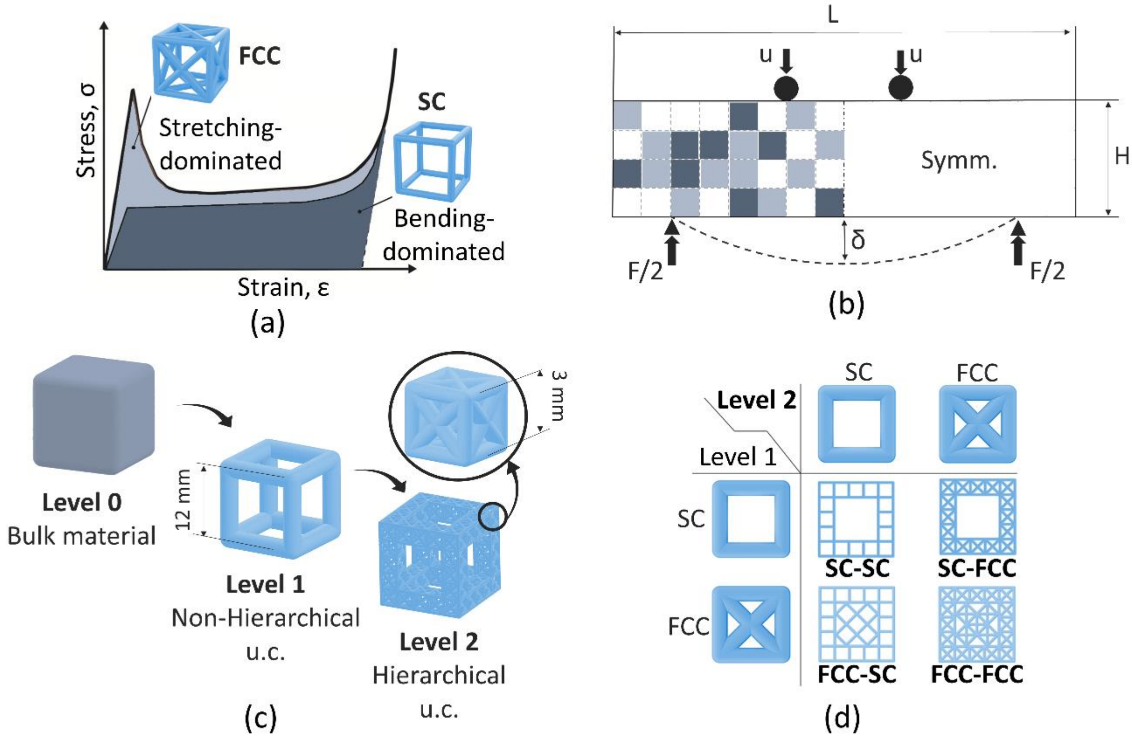

Figure 2 - Representation of the modeling process of lattice structures. (a) Selection of u.c. according to their mechanical behavior and geometric compatibility. (b)Voxelization of the design space consisting of a four-point bending beam (symmetrical with respect to the midplane). The design space has square cross section and nominal dimensions L = 192 mm and H = 48 mm and is subjected to a 4PB load. F represents the reaction force, u the imposed

displacement, and δ the maximum specimen deflection. (c) Representation of the design process of hierarchical lattice u.c.. The edge length dimensions used for this study are equal to 12 mm and to 3 mm for the NH-u.c. and the H-u.c. respectively. (d) Schematization of the building rationale used to generate the hierarchical (or level 2) u.c..

The NHL-structure is obtained by replacing the bulk beam material with the selected u.c., voxel by voxel. In the HL-structure, each voxel is made by hierarchical u.c. (i.e., level 2), as shown in figure 2c. figure 2d shows the H-u.c. that are obtained from all the possible combinations of FCCs and SCs on a smaller length scale.

As a convention, the names of the H-u.c. are defined through acronyms consisting of two parts "x-y": the first one, "x", describing the level 1 u.c., the second one, "y", describing the level 2 u.c. (figure 2d). The minimum dimensions of the struts of the lattice u.c. are chosen in compliance with the technological constraints associated with a Prusa i3 MK3S Original kit 3D printer mounting a 0.4 mm nozzle that emerged while printing with PLA several models as proof-of-concept. The u.c. edges length are fixed at 12 and 3 mm for level 1 and 2, respectively (figure 2c). To study the combined effect of hierarchy and structural heterogeneity, different topologies are exploited as population strategies for the design space. Four different NHL-structures are studied: i) SC-structure, made of only SC u.c., ii) FCC-structure, made of only FCC u.c., iii) a "sandwich" like architecture, called SAND-structure, and iv) a topologically optimized one, named TOPO-structure. The i)-ii) structures are homogenous lattice structures consisting of a unique type of u.c., whereas the iii)-iv) structures are obtained by combining the SC and FCC u.c. into heterogeneous architectures. The SAND- and TOPO-structure configurations are designed according to the optimization strategies commonly used to achieve optimal mechanical response of structures under bending loading conditions. In particular, the SAND-model is designed to emulate the structure of well-known sandwich panels, where rigid skins and lightweight core are combined to increase the flexural stiffness-to-weight ratio. The TOPO-, on the other hand, is made from the results of a topological optimization on a 4PB beam that maximizes flexural stiffness, replacing areas where bulk material is left with FCC u.c., well-known for their structural efficiency, while areas where bulk material is removed, filled with SC cells, well-known for their lightweight. The NHL-structures schematization is reported in figure 3a. The combination of these four topologies with the hierarchy (*i.e.*, H-u.c.) led to the definition of twelve HL-structures. A schematic representation of the TOPO HL-beams is provided in figure 3b. All the structure analyzed in this study are included in Supporting Information (figure S1-S2). The structure names are composed by two parts: the first describes the level-1 population strategy, while the second describes the level-2 population strategy.

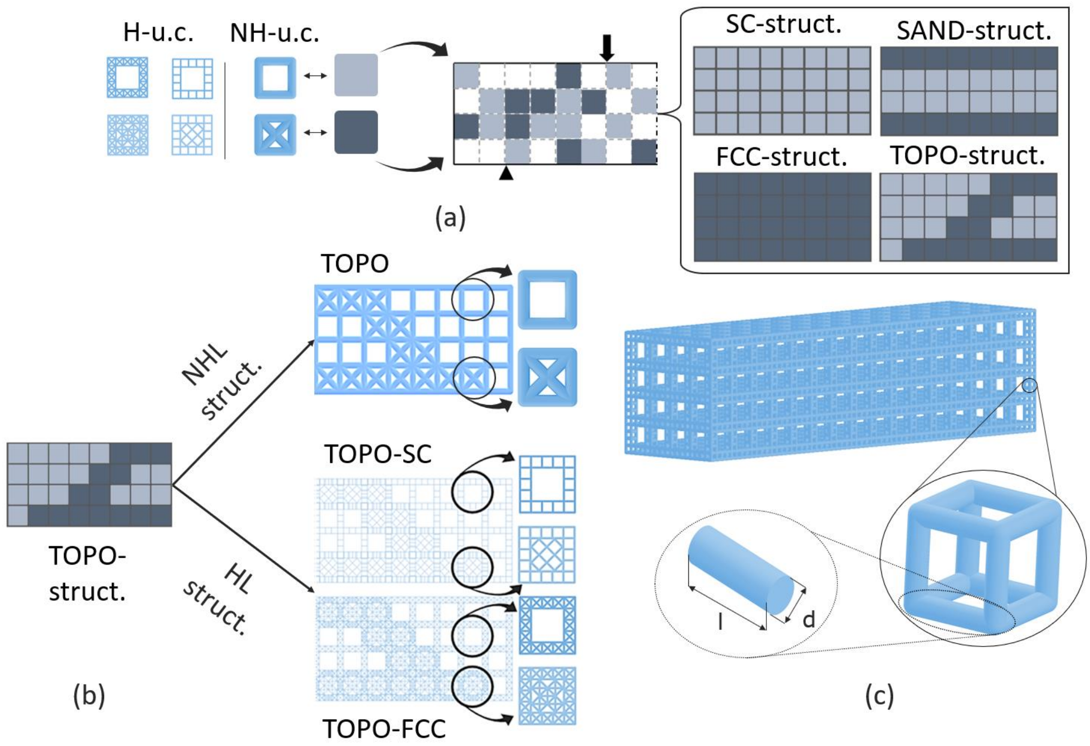

Figure 3 - (a) Representation of the four different design space population strategies. (b) Example of the lattice structures derived from a specific population strategy: TOPO-structures. (c) 3D representation of a hierarchical lattice structure and u.c. strut diameter, d, and length, l definition.

2.2 Numerical simulations

To study the mechanical behavior of the architected lattice structures, numerical simulations are performed using ANSYS Mechanical APDL. This is essential for the formulation of customized calculation routines (*i.e.*, macros) capable of correctly defining u.c. and different hierarchical lattice topologies, and analyzing their structural behavior in an automated manner. Indeed, by programming the FE analysis input file, the geometries of the lattice models are built parametrically, using 3D FE beam-type (BEAM 188 with KEYOPT(3)=0 in the Ansys MAPDL element library). An iterative cycle is set up to automatically compute the solution of the different designs. The use of beam elements, despite allowing only a simplified representation of the real phenomena to be studied, allows for the evaluation of more than 80 different geometric configurations in a reasonable time frame and with limited computational effort. The exploitation of geometrical symmetry, material properties, and boundary conditions, present in all the designed lattice models, allow us to further speed up the analyses. Simulations are performed in displacement control, assigning a negative deflection of 0.3 mm to the nodes of the finite element models located at the required bending pins for a four-point experimental test. The minimum size of the finite element mesh is defined according to a convergence analysis. Specifically, in the NHL-structures each strut is discretized into ten beam elements, while for the HL-structures each strut of the smallest u.c. is constructed by exploiting two FEs. A homogeneous and isotropic linear elastic model, calibrated on the base of experimentally determined properties of a commercial 3D printing PLA, is used for the material model.

2.3 Data analyses

The architected lattice structures are analyzed by varying the *s.r.* and, consequently, the relative density (ρ_{rel}), respectively defined as follows:

$$s.r. = \frac{d}{l} \tag{1}$$

$$\rho_{rel} = \frac{\rho^*}{\rho_{bulk}} = f\left(\frac{D}{L}\right) \tag{2}$$

where d is the diameter of the struts of the smallest u.c., l is the side length of the smallest u.c. (see figure 3c), ρ^* is the density of the lattice material considering the apparent volume, and ρ_{bulk} is the bulk density of the base material. Once fixed the u.c. edge length, we set the *s.r.* range from 0.15 to 0.45, then the strut diameters are calculated accordingly. The same *s.r.* are used for both the H-u.c. and the NH-u.c.. This strategy for defining the *s.r.* is consistent with previous studies [33]. The performance of the structures is measured through the relative modulus (E_{rel}) and the stiffness-to-weight ratio (*s.t.w.*), that are among the most used parameters for characterizing lattice materials according to literature [36]. Relative modulus of elasticity is defined as:

$$E_{rel} = \frac{E^*}{E_{bulk}} \tag{3}$$

where E^* is the apparent modulus of the lattice material and E_{bulk} is the Young's modulus of the bulk material. The *s.t.w.* ratio, on the other hand, is defined as:

$$s.t.w. = \frac{F}{\delta \cdot W} \tag{4}$$

where, with reference to a four-point bending beam configuration, F is the force exerted by the bending pins, δ is the maximum deflection experienced by the specimen, and W is the structure weight. Having introduced E_{rel} and ρ_{rel} we can define the scaling law, characterizing the lattice material elastic behavior, as follows:

$$E_{rel} \propto \rho_{rel}^n \tag{5}$$

Generally, the scaling laws are represented in a log-log diagram, where the exponent, *n*, becomes the slope of the scaling laws.

3. Results

In this section, we discuss the results obtained for the NHL-structures and HL-structures, by comparing the flexural properties of the structures (i.e., *s.t.w.* and E_{rel}) as a function of the *s.r.* and ρ_{rel}.

3.1 Topology effects on NHL-structures

Figure 4a,b shows the results of the NHL-structures. In particular, SC and SAND structures have comparable performance in terms of numerical values, as well as FCC and TOPO. While the FCC and the SAND have higher *s.t.w.* for low *s.r.* with respect to the TOPO and SC, respectively, the trend is inverted for higher *s.r.*. In fact, for *s.r.* included in the 0.30-0.45 range the SC and the TOPO show higher *s.t.w.*. Also, comparing the performances of the FCC and SC we can see that for low *s.r.* there is a large difference in terms of *s.t.w.*: at *s.r.*=0.15 the FCC-structure has a 5-fold *s.t.w.* compared to SC. This gap is dramatically reduced for higher *s.r.*: at *s.r.*=0.45 the FCC is about 30% higher. The scaling laws in figure 4b, instead, highlight the different structural performance. As expected, the homogeneous SC structure shows a more bending-dominated behavior (n=1.7), while the FCC and the TOPO show a stretching-dominated behavior (n=1.1 and n=1.2, respectively). The SAND structure has an intermediate behavior (n=1.4).

3.2 Topology effects on HL-structures

For the HL-structures the results are grouped by the topology of level 1. In figure 4c,d there are five different curves, for each plot, while for the plots depicted in figure 4e,f there are only three curves. The colored curves represent the HL-structures (each color represents a different topology at level 2). The black curve represents the NHL-structures (at level 1) that will be used as benchmark. Figure 4c shows the result for the SC HL-structures. All the curves are approximately parallel to each other and the overall behavior is bending-dominated, with an average $\bar{n} = 1.8$. This means that the dominant level is the macroscopic one, level 1. More details are provided in Table S1 (Supporting Information). Moreover, the introduction of geometrical complexity in terms of hierarchy does not produce any beneficial effects in the material mechanical response. Only the SC-SC structure matches the performance of the SC NHL-structures and extends the range of ρ_{rel} to lower values.

Looking at the result for the FCC HL-structures, figure 4d, it is possible to notice that the overall behavior is again driven by level 1, being $\bar{n} = 1.20$ (stretching-dominated). Also, the FCC HL-structures shows worse performance with respect to FCC NHL-structure. On the contrary, the FCC HL-structures shows better performances, for the same ρ_{rel}, with respect to the SC HL-structures. figure 4e shows the outcome of the SAND HL-structures. In this case, the trend is different from the previous ones: the HL-structures outperforms the NHL-structure. The trend changes with hierarchy, becoming more stretching-dominated (the slopes are lower). The SAND-SC structure has a slope similar to the SAND one but shows higher E_{rel} for the same ρ_{rel}. Also, the SAND-FCC is outperforming the SAND for low values of ρ_{rel}. Then, due to the more stretching-dominated behavior of the NHL-structure, the latter shows better performances, increasing the ρ_{rel}. The result for the TOPO HL-structures in figure 4f shows that there is no hierarchy-induced mechanical improvement. Also in this case, the overall behavior is mainly stretching-dominated ($\bar{n} = 1.20$). By analyzing the scaling laws the HL-structures having homogeneous SC level 2, we can see a different behavior depending on the topology of level 1. More precisely, if the level 1 shows a more bending-dominated behavior (as for the SC and SAND structures) the introduction of the SC at level 2 makes the HL-structures more stretching-dominated. While, if level 1 has a stretching-dominated behavior, the introduction of the bending-dominated unit cell at level 2 makes the HL-structures more bending dominated.

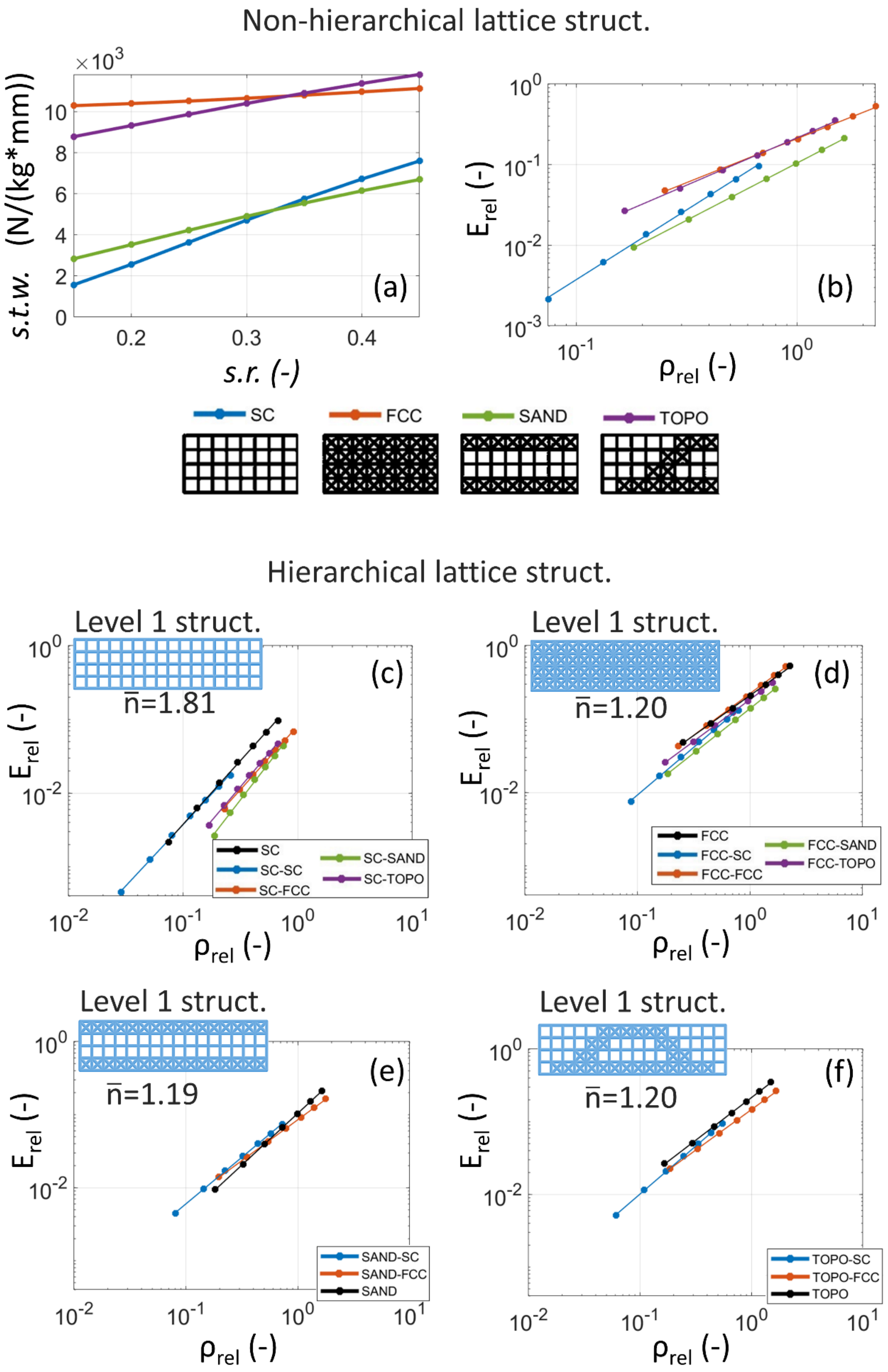

Figure 4 - Non-hierarchical lattice structures results: (a) Stiffness-to-weight ratio vs slenderness ratio; (b) Relative modulus vs relative density (scaling law). Hierarchical lattice structures results: (c)-(f) scaling laws of the hierarchical lattice structures. Panel (b)-(f) are in log-log scale. Each color corresponds to a different topology, according to the legend.

4. Discussions

NHL-structures demonstrate significantly different mechanical behaviors: all four topologies show an increase in stiffness as the *s.r.* of the u.c. struts (and thus their diameter) increases, but they fall into two different clusters. FCC and TOPO structures are much more efficient–in terms of stiffness–than SC and SAND structures. Indeed, the former, show higher performance than the latter, at a given *s.r.*. The difference between SC and FCC structures confirms the theoretical scaling laws. The difference between SAND and TOPO structures, on the other hand, allows us to highlight the fundamental role of structural heterogeneity on the performance of NHL-structures and paves the way for the optimization of the analyzed models. Heterogeneous structures, such as SAND and TOPO, show hybrid behavior compared to homogeneous models (i.e., those made of only stretching- or bending-dominated u.c.). Indeed, their scaling laws are interposed between those of the FCC and those of the SC structures. The TOPO structure, however, is much more efficient than the SAND structure, showing performance that–for high *s.r.* values–far exceeds that of the FCC structure. This means that, for a given number of SC and FCC cells combined together to build heterogeneous lattice structures, applying topological optimization logic at level 1 can yield hybrid lattice structures with better performance than homogeneous stretching-dominated ones. Also, considering the difference in the performance of SC and FCC structures, we can state that an optimized structure would have not only heterogeneous u.c. within the design space, but also varying *s.r.*, depending on the structural behavior of the u.c. (e.g., bending-dominated u.c. with high *s.r.* and stretching-dominated u.c. with low *s.r.*). A first attempt in this direction was done by the authors, finding that variable *s.r.* structures can improve the performance with respect to constant *s.r.* structures. Further details are provided in Supporting Information, figure S4. The same *s.r.* differentiation strategy, applied to homogeneous non-hierarchical structures, would not lead to the same benefits. Indeed, the FCC structure performance is not affected by the *s.r.* and the SC structure is weaker than the other configurations, regardless of *s.r.* value.

HL-structures are generally less efficient than the corresponding NHL-structures, in terms of specific mechanical performance. Regardless the adopted design space population strategy, the elastic behavior of HL-structures is found to be strongly dependent on the type of structural organization present at level 1 (Table S1 Supporting Information), and we do not observe significant variations induced by the type of u.c. at level 2. Only a few exceptional cases show hierarchy-improved mechanical performance of the non-hierarchical lattice structures (e.g., the hierarchical SAND structures and the FCC-FCC structure), but there is no clear evidence to define sharp design guidelines for effective exploitation of the multiscale modeling logic used in this study. What we observe runs against the trend of previous findings in the literature [16], [28]–[34]. Indeed, a recurring outcome in research on HL-materials is that bending-dominated structures can benefit from hierarchy if stretching-dominated substructures are introduced within them. In this study, this evidence is not clear. This may be due to the different loading scenario, and possible edge effects due to the low number of u.c. used to generate the various lattice structure models. Nevertheless, the mechanical behavior of the analyzed lattice structures is comparable to that of other lattice materials (figure 5). Yet, an open question is to optimize the structural organization at level 2, by exploiting design logics similar to those discussed above for NHL-structure models, and to introduce periodic boundary condition to overcome the edge effect limitations.

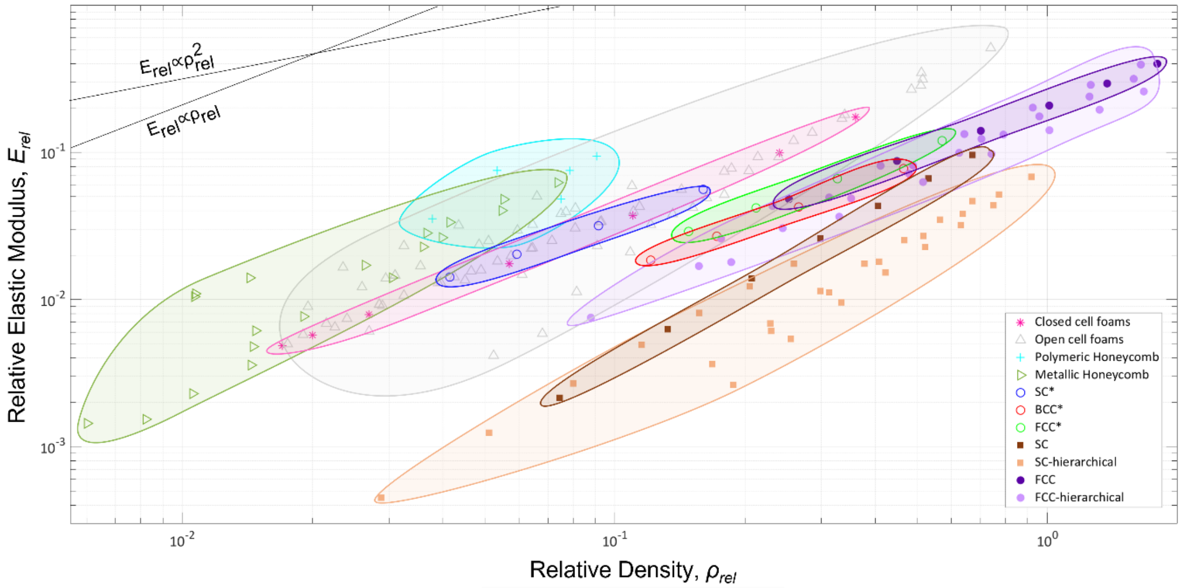

Figure 5 - Relative elastic modulus vs relative density bubble chart: results comparison between previous studies and results obtained in this research work. Data referenced by the asterisk (*) were taken from [37].

5. Concluding remarks and outlook

In our work, we analyze different types of 3D lattice structures under bending loading scenario: four types of NHL-structures, characterized by different population strategies and twelve types of HL-structures. The structures are obtained by combining together two different types of lattice u.c., characterized by stretching- and bending-dominated behaviors. The lattice structures are analyzed by varying the *s.r.* of the smallest u.c.. The outcome of this study shows that introducing structural heterogeneity, by combining different u.c. types, can be beneficial in terms of mechanical properties and this improvement can be further extended by customizing the *s.r.* for the different type of u.c.. Conversely, structural hierarchy does not necessary lead to significant improvements in the deformation behavior for the lattice structures analyzed. Nevertheless, hierarchy allows one to extend the range of relative densities to lower values, while maintaining comparable mechanical properties, which is the key-point of the lightweight design strategy. Furthermore, for the same mechanical performance, the geometrical features of HL-structures differ considerably from those of NH- ones (e.g., significant changes in surface-to-volume ratios), paving the way for new applications of such materials in novel fields, from heat exchangers, to mechanical filters, and tissue regeneration scaffolds. This could be possible also thanks to additive manufacturing, which allows one to overcome manufacturing limitations of conventional fabrication techniques. This research mainly focused on the elastic properties of hierarchical lattice structures, while their failure modes and inelastic behaviors are under investigation. Future research will involve an experimental campaign, through 3D-printing and mechanical testing of selected lattice structures, to validate the numerical models and provide a more comprehensive understanding of the deformation and failure mechanisms.

References

[1] T. A. Schaedler and W. B. Carter, "Architected Cellular Materials," *Annu. Rev. Mater. Res.*, vol. 46, no. April, pp. 187–210, 2016, doi: 10.1146/annurev-matsci-070115-031624.

[2] F. Tamburrino, S. Graziosi, and M. Bordegoni, "The design process of additively manufactured mesoscale lattice structures: A review," *J. Comput. Inf. Sci. Eng.*, vol. 18, no. 4, pp. 1–16, 2018, doi: 10.1115/1.4040131.

[3] J. Plocher and A. Panesar, "Review on design and structural optimisation in additive manufacturing: Towards next-generation lightweight structures," *Materials and Design*, vol. 183. Elsevier Ltd, p. 108164, Dec. 05, 2019, doi: 10.1016/j.matdes.2019.108164.

[4] M. S. Pham, C. Liu, I. Todd, and J. Lertthanasarn, "Damage-tolerant architected materials inspired by crystal microstructure," *Nature*, vol. 565, no. 7739, pp. 305–311, 2019, doi: 10.1038/s41586-018-0850-3.

[5] R. Manno, W. Gao, and I. Benedetti, "Engineering the crack path in lattice cellular materials through bio-inspired micro-structural alterations," *Extrem. Mech. Lett.*, vol. 26, pp. 8–17, 2019, doi: 10.1016/j.eml.2018.11.002.

[6] M. Benedetti, A. du Plessis, R. O. Ritchie, M. Dallago, S. M. J. Razavi, and F. Berto, "Architected cellular materials: A review on their mechanical properties towards fatigue-tolerant design and fabrication," *Mater. Sci. Eng. R Reports*, vol. 144, p. 100606, 2021, doi: 10.1016/j.mser.2021.100606.

[7] X. Xia, C. M. Spadaccini, and J. R. Greer, "Responsive materials architected in space and time," *Nat. Rev. Mater.*, vol. 0123456789, 2022, doi: 10.1038/s41578-022-00450-z.

[8] M. F. Gibson, Lorna J., Ashby, *Cellular Solids. Structure and Propertes.* Cambridge University Press, 2014.

[9] M. F. Ashby, "The properties of foams and lattices," *Philos. Trans. R. Soc. A Math. Phys. Eng. Sci.*, vol. 364, no. 1838, pp. 15–30, 2006, doi: 10.1098/rsta.2005.1678.

[10] J. Somnic and B. W. Jo, "Homogenization Methods of Lattice Materials," *Encyclopedia*, vol. 2, no. 2, pp. 1091–1102, 2022, doi: 10.3390/encyclopedia2020072.

[11] M. Kadic, G. W. Milton, M. van Hecke, and M. Wegener, "3D metamaterials," *Nat. Rev. Phys.*, vol. 1, no. 3, pp. 198–210, 2019, doi: 10.1038/s42254-018-0018-y.

[12] X. Yu, J. Zhou, H. Liang, Z. Jiang, and L. Wu, "Mechanical metamaterials associated with stiffness, rigidity and compressibility: A brief review," *Prog. Mater. Sci.*, vol. 94, pp. 114–173, 2018, doi: 10.1016/j.pmatsci.2017.12.003.

[13] Y. Liu, G. Zheng, N. Letov, and Y. F. Zhao, "A Survey of Modeling and Optimization Methods for Multi-Scale Heterogeneous Lattice Structures," *J. Mech. Des. Trans. ASME*, vol. 143, no. 4, 2021, doi: 10.1115/1.4047917.

[14] E. D. Sanders, A. Pereira, and G. H. Paulino, "Optimal and continuous multilattice embedding," 2021. [Online]. Available: http://advances.sciencemag.org/.

[15] C. Pan, Y. Han, and J. Lu, "Design and optimization of lattice structures: A review," *Appl. Sci.*, vol. 10, no. 18, pp. 1–36, 2020, doi: 10.3390/APP10186374.

[16] S. Banerjee, "On the mechanical properties of hierarchical lattices," *Mech. Mater.*, vol. 72, pp. 19–32, 2014, doi: 10.1016/j.mechmat.2014.01.009.

[17] X. Zheng *et al.*, "Multiscale metallic metamaterials," *Nat. Mater.*, vol. 15, no. 10, pp.

1100–1106, 2016, doi: 10.1038/nmat4694.

[18] Z. Wu, L. Xia, S. Wang, and T. Shi, "Topology optimization of hierarchical lattice structures with substructuring," *Comput. Methods Appl. Mech. Eng.*, vol. 345, pp. 602–617, 2019, doi: 10.1016/j.cma.2018.11.003.

[19] L. Musenich and F. Libonati, "Damage and Failure Mechanisms of Biological Materials," in *Reference Module in Materials Science and Materials Engineering*, Elsevier, 2022.

[20] Z. Liu, M. A. Meyers, Z. Zhang, and R. O. Ritchie, "Functional gradients and heterogeneities in biological materials: Design principles, functions, and bioinspired applications," *Prog. Mater. Sci.*, vol. 88, pp. 467–498, 2017, doi: 10.1016/j.pmatsci.2017.04.013.

[21] W. Huang *et al.*, "Multiscale Toughening Mechanisms in Biological Materials and Bioinspired Designs," *Adv. Mater.*, vol. 31, no. 43, pp. 1–37, 2019, doi: 10.1002/adma.201901561.

[22] Z. Liu, Z. Zhang, and R. O. Ritchie, "Structural Orientation and Anisotropy in Biological Materials: Functional Designs and Mechanics," *Adv. Funct. Mater.*, vol. 30, no. 10, pp. 1–17, 2020, doi: 10.1002/adfm.201908121.

[23] Z. Liu *et al.*, "Adaptive structural reorientation: Developing extraordinary mechanical properties by constrained flexibility in natural materials," *Acta Biomater.*, vol. 86, pp. 96–108, 2019, doi: 10.1016/j.actbio.2019.01.010.

[24] Lakes R. S., "Materials with structural hierarchy," *Nature*, vol. 361, pp. 511–515, 1993.

[25] G. B. Olson, "Computational design of hierarchically structured materials," *Science*, vol. 277, no. 5330, pp. 1237–1242, 1997, doi: 10.1126/science.277.5330.1237.

[26] V. Perricone, C. Santulli, F. Rendina, and C. Langella, "Organismal design and biomimetics: A problem of scale," *Biomimetics*, vol. 6, no. 4, 2021, doi: 10.3390/biomimetics6040056.

[27] S. C. L. Fischer, L. Hillen, and C. Eberl, "Mechanical metamaterials on the way from laboratory scale to industrial applications: Challenges for characterization and scalability," *Materials (Basel).*, vol. 13, no. 16, pp. 1–16, 2020, doi: 10.3390/MA13163605.

[28] A. Ajdari, B. H. Jahromi, J. Papadopoulos, H. Nayeb-Hashemi, and A. Vaziri, "Hierarchical honeycombs with tailorable properties," *Int. J. Solids Struct.*, vol. 49, no. 11–12, pp. 1413–1419, 2012, doi: 10.1016/j.ijsolstr.2012.02.029.

[29] R. Oftadeh, B. Haghpanah, D. Vella, A. Boudaoud, and A. Vaziri, "Optimal fractal-like hierarchical honeycombs," *Phys. Rev. Lett.*, vol. 113, no. 10, pp. 1–5, 2014, doi: 10.1103/PhysRevLett.113.104301.

[30] R. Oftadeh, B. Haghpanah, J. Papadopoulos, A. M. S. Hamouda, H. Nayeb-Hashemi, and A. Vaziri, "Mechanics of anisotropic hierarchical honeycombs," *Int. J. Mech. Sci.*, vol. 81, pp. 126–136, 2014, doi: 10.1016/j.ijmecsci.2014.02.011.

[31] A. Vigliotti and D. Pasini, "Mechanical properties of hierarchical lattices," *Mech. Mater.*, vol. 62, pp. 32–43, 2013, doi: 10.1016/j.mechmat.2013.03.003.

[32] L. R. Meza, A. J. Zelhofer, N. Clarke, A. J. Mateos, D. M. Kochmann, and J. R. Greer, "Resilient 3D hierarchical architected metamaterials," *Proc. Natl. Acad. Sci. U. S. A.*, vol. 112, no. 37, pp. 11502–11507, 2015, doi: 10.1073/pnas.1509120112.

[33] Y. Sha, L. Jiani, C. Haoyu, R. O. Ritchie, and X. Jun, “Design and strengthening mechanisms in hierarchical architected materials processed using additive manufacturing,” *Int. J. Mech. Sci.*, vol. 149, no. July, pp. 150–163, 2018, doi: 10.1016/j.ijmecsci.2018.09.038.

[34] V. S. Deshpande, M. F. Ashby, and N. A. Fleck, “Foam topology: Bending versus stretching dominated architectures,” *Acta Mater.*, vol. 49, no. 6, pp. 1035–1040, 2001, doi: 10.1016/S1359-6454(00)00379-7.

[35] D. Sen and M. J. Buehler, “Structural hierarchies define toughness and defect-tolerance despite simple and mechanically inferior brittle building blocks,” *Sci. Rep.*, vol. 1, pp. 1–9, 2011, doi: 10.1038/srep00035.

[36] S. Graziosi, F. M. Ballo, F. Libonati, and S. Senna, “3D printing of bending-dominated soft lattices: numerical and experimental assessment,” *Rapid Prototyp. J.*, vol. 28, no. 11, pp. 51–64, 2022, doi: 10.1108/RPJ-03-2022-0095.

[37] F. Libonati, S. Graziosi, F. Ballo, M. Mognato, and G. Sala, “3D-Printed Architected Materials Inspired by Cubic Bravais Lattices,” *ACS Biomater. Sci. Eng.*, 2021, doi: 10.1021/acsbiomaterials.0c01708.